

April 2021

Dear Researcher,

Thank you for downloading and using this article from the *Journal of Environmental Quality* (JEQ). A bimonthly journal published jointly by the ASA, CSSA, and SSSA, JEQ presents original research, reviews and analyses, and environmental issue articles addressing anthropogenic impacts on water, soil, and the atmosphere.

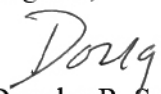
Publishing high quality research articles such as this one would not be possible without individuals offering their time and talents by volunteering to review. I am asking you to extend your help to our journal and in turn benefit the research community through manuscript review.

Registering to review is easy and helps us invite you when a manuscript aligning with your key study areas requires your subject matter expertise. You're under no obligation, but the value your review adds to the JEQ corpus is indispensable. You don't need to be a seasoned researcher to volunteer. We welcome early career researchers, postdocs, etc.; our editorial board and experienced staff are here to guide you through the process.

Browse to the JEQ ScholarOne submission site at <https://mc.manuscriptcentral.com/jeq> now and create an account with keywords to help us match you with the right submissions. If you already have an account, please take a moment to update your keywords.

Again, thank you for using our journal and sharing your expertise with the research community. If you have any questions or want more information, please contact the JEQ Editorial Office at jeq@sciencesocieties.org.

Regards,


Douglas R. Smith, Editor
Journal of Environmental Quality

TECHNICAL REPORTS

Bioremediation and Biodegradation

Microbial controls on net production of nitrous oxide in a denitrifying woodchip bioreactor

Albin Nordström¹  | Maria Hellman² | Sara Hallin² | Roger B. Herbert¹ 

¹ Dep. of Earth Sciences, Uppsala Univ., Villavägen 16, Uppsala SE-752 36, Sweden

² Dep. of Forest Mycology and Plant Pathology, Swedish Univ. of Agricultural Sciences, Box 7026, Uppsala SE-750 07, Sweden

Correspondence

Roger B. Herbert, Dep. of Earth Sciences, Uppsala Univ., Villavägen 16, SE-752 36, Uppsala, Sweden.

Email: roger.herbert@geo.uu.se

Assigned to Associate Editor Michelle Soupier.

Funding information

VINNOVA, Grant/Award Number: 2014-011334; Luossavaara-Kiirunavaara Aktieföretag (LKAB)

Abstract

Denitrifying woodchip bioreactors are potential low-cost technologies for the removal of nitrate (NO_3^-) in water through denitrification. However, if environmental conditions do not support microbial communities performing complete denitrification, other N transformation processes will occur, resulting in the export of nitrite (NO_2^-), nitrous oxide (N_2O), or ammonium (NH_4^+). To identify the factors controlling the relative accumulation of NO_2^- , N_2O , and/or NH_4^+ in denitrifying woodchip bioreactors, porewater samples were collected over two operational years from a denitrifying woodchip bioreactor designed for removing NO_3^- from mine water. Woodchip samples were collected at the end of the operational period. Changes in the abundances of functional genes involved in denitrification, N_2O reduction, and dissimilatory NO_3^- reduction to NH_4^+ were correlated with porewater chemistry and temperature. Temporal changes in the abundance of the denitrification gene *nirS* were significantly correlated with increases in porewater N_2O concentrations and indicated the preferential selection of incomplete denitrifying pathways ending with N_2O . Temperature and the total organic carbon/ NO_3^- ratio were strongly correlated with NH_4^+ concentrations and inversely correlated with the ratio between denitrification genes and the genes indicative of ammonification ($\Sigma\text{nir}/\text{nrfA}$), suggesting an environmental control on NO_3^- transformations. Overall, our results for a denitrifying woodchip bioreactor operated at hydraulic residence times of 1.0–2.6 d demonstrate the temporal development in the microbial community and indicate an increased potential for N_2O emissions with time from the denitrifying woodchip bioreactor.

1 | INTRODUCTION

Denitrifying fixed-bed bioreactors are low-cost technologies for the removal of nitrate (NO_3^-) from water, which passes

through an organic porous material, supplying electrons for the reduction of NO_3^- to nitrogen gas (N_2) (Schipper, Robertson, Gold, Jaynes, & Cameron, 2010). Woodchips are typically used due to their high permeability, moderate reactivity, and capability of providing a carbon (C) and energy source for denitrification (Cameron & Schipper, 2010; Robertson, 2010; Schipper et al., 2010). However, the release of other nitrogen (N) species (nitrite [NO_2^-], nitric oxide [NO], and the greenhouse gas nitrous oxide [N_2O]) from intermediate steps during denitrification is a potential drawback of

Abbreviations: DNRA, dissimilatory NO_3^- reduction to ammonium; DWB, denitrifying woodchip bioreactor; HRT, hydraulic residence time; NMDS, nonmetric multidimensional scaling; PCR, polymerase chain reaction; qPCR, quantitative polymerase chain reaction; TOC, total organic carbon.

This is an open access article under the terms of the [Creative Commons Attribution](https://creativecommons.org/licenses/by/4.0/) License, which permits use, distribution and reproduction in any medium, provided the original work is properly cited.

© 2020 The Authors. *Journal of Environmental Quality* published by Wiley Periodicals LLC on behalf of American Society of Agronomy, Crop Science Society of America, and Soil Science Society of America

denitrifying woodchip bioreactors (DWBs) (Davis, Martin, Moorman, Isenhardt, & Soupir, 2019; Feyereisen et al., 2016). Up to 10% of the reduced NO_3^- is exported as N_2O from DWBs (Davis et al., 2019; Elgood, Robertson, Schiff, & Elgood, 2010; Feyereisen et al., 2016; Greenan, Moorman, Kaspar, Patkin, & Jaynes, 2006; Warneke et al., 2011b). The release of these compounds is affected by temperature, NO_3^- concentration, dissolved oxygen concentration (Elgood et al., 2010; Griebmeier, Bremges, McHardy, & Gescher, 2017), and the functional communities involved in the production or reduction of these compounds (Warneke et al., 2011b).

Denitrifiers compete with bacteria performing dissimilatory NO_3^- reduction to ammonium (NH_4^+) (DNRA) for NO_3^- , and the outcome of this competition determines if NO_3^- is removed as a gaseous N species or is converted to aqueous NH_4^+ , thereby affecting the overall N removal capacity of the DWB. The availability of organic C in relation to NO_3^- (C/ NO_3^- ratio) has been shown to control this competition, with high C/ NO_3^- ratios favoring DNRA (Kraft et al., 2014; Van Den Berg, Van Dongen, Abbas, & Van Loosdrecht, 2015; Yoon, Cruz-García, Sanford, Ritalahti, & Löffler, 2015) and low ratios favoring denitrification, which includes an increased risk for the net production of N_2O (Pan, Ni, Bond, Ye, & Yuan, 2013). This is not only because more N_2O is produced during denitrification than DNRA but also because denitrification can terminate with N_2O under NO_3^- -rich conditions (Felgate et al., 2012). For some denitrifiers, N_2O is always the end product because they do not have the genetic repertoire needed to further reduce N_2O to N_2 and because they, as well as nondenitrifying N_2O reducers, also affect the net N_2O emissions (Graf, Jones, & Hallin, 2014; Hallin, Philippot, Löffler, Sanford, & Jones, 2018; Jones et al., 2014). In DWBs, C availability is controlled by woodchip degradation, and the relative availability of different C substrates may change throughout DWB operations (Griebmeier & Gescher, 2018; Griebmeier et al., 2017; Nordström & Herbert, 2018). It can therefore be expected that differences in relative abundances of the functional groups involved in the different N transforming processes develop over time during DWB operation. The proportion between these functional groups ultimately controls the export of N species from DWBs, but little is known about the temporal development of the N-transforming community and the associated temporal changes in the production of NO_2^- , N_2O , and NH_4^+ in DWBs.

In this study, temporal and spatial changes of the abundances of functional groups performing denitrification and DNRA in the porewater were studied with the objectives to relate these patterns with changes in the concentrations of NO_2^- , N_2O , and NH_4^+ in the porewater and overall reactor performance in a previously described DWB (Nordström & Herbert, 2018). We hypothesized that temporal and spatial changes in the genetic potential for denitrification and DNRA, determined as abundances of functional genes in den-

Core Ideas

- A high degree of spatial and temporal variability for functional gene abundances was noted in porewater.
- Temperature dependence was exhibited especially for the gene *nrfA*.
- N_2O production correlated with *nirS* abundance and $\Sigma\text{nir}/\Sigma\text{nosZ}$ ratio.
- TOC/ NO_3^- ratio positively correlated with *nrfA* abundance and NH_4^+ concentration.
- A truncated denitrification pathway was promoted with time in the bioreactor.

itrifying and DNRA bacteria, control concentrations of NO_2^- , N_2O , and NH_4^+ and that their abundances are a consequence of changes in C/ NO_3^- ratios. Because the porewater community is more easily sampled for temporal studies than the woodchip-associated community, we primarily monitored the development of the N-reducing community in the porewater. However, for the last sampling episode, we compared the spatial distribution of the abundance of denitrifying and DNRA bacteria in the woodchip matrix with their spatial distribution in porewater.

2 | MATERIALS AND METHODS

2.1 | Study site and DWB system

The subsurface DWB described by Nordström and Herbert (2018) was constructed at the Kiruna iron ore mine, northern Sweden (67°51' N, 20°13' E), with the purpose to reduce NO_3^- concentrations in mine and process water originating from the use of ammonium nitrate-based explosives. For this study, samples from the inlet, outlet, and five porewater sampling points along the bottom centerline of the DWB were used (Supplemental Figure S1).

The DWB was filled with decorticated pine woodchips. To increase the initial abundance of denitrifying microorganisms, digested sewage sludge mixed with water was added while the DWB was filled with woodchips. The center areas of the DWB were capped by glacial till (Supplemental Figure S1) with the intention to restrict oxygen diffusion into the DWB.

Mine drainage from the clarification pond at the mine site was pumped to the DWB, where it entered through a perforated drainage pipe near the surface of the DWB and extending across its width. The hydraulic residence time (HRT) of the DWB was adjusted several times during the operational periods by changing the pump discharge

(Supplemental Table S1), with 2.6 d being the most common HRT (varying between 1 and 2.6 d). The choice of HRT was based on a previous laboratory-scale experiment where relatively long HRTs at low temperature provided nearly complete removal of NO_3^- (Nordström & Herbert, 2017). The DWB was operated for two consecutive field seasons: 22 June to 21 Nov. 2015 (Days 0–151) and 9 May to 21 Oct. 2016 (Days 322–490), referred to as the first and second operational year, respectively.

2.2 | DWB sampling

2.2.1 | Water sampling

Porewater, inlet water, and outlet water were sampled once a month (referred to as “profile sampling”) to analyze water chemistry (Nordström & Herbert, 2018). Briefly, a peristaltic pump was used for porewater sampling, and the first ~2 L of water was discarded prior to sample collection to ensure a representative sample. Inlet and outlet water was grab-sampled. For analyses of microbial communities involved in N transformation processes, water sampled on Days 57, 85, 113, 365, 400, 428, 456, and 477 was filtered using Sterivex filter units, with 0.22- μm Millipore Express polyethersulfone membranes, attached to 60-ml syringes. Inlet water samples from Days 57 and 85 were discarded because of technical problems during sampling. Between 540 and 1,680 ml of water (average, 990 ml) was required to saturate the Sterivex filter units. The syringes were rinsed in sample water three times prior to filtration, and new polyvinyl chloride plastic tubing for the peristaltic pump was used for each sample. The Sterivex filter units were stored on ice for ~6 h following collection and frozen at -20°C until DNA extraction.

Denitrifying woodchip bioreactor porewater temperature was obtained from thermistors attached to porewater sampling points at the base of the DWB.

2.2.2 | Woodchips and sewage sludge media

Sewage sludge samples used as inoculum were collected in sterile 50-ml plastic tubes at the time of DWB construction and frozen at -20°C until analysis. Woodchips were sampled following the termination of DWB operations (Day 490). The sampling focused on the deepest regions of the DWB because a previous DWB study indicated a significantly greater abundance of 16S rRNA, *nirS*, *nirK*, and *nosZI* genes at the greatest depths in a DWB (Herbert, Winbjörk, Hellman, & Hallin, 2014). Water was drained from the DWB, and transverse trenches were excavated at 2.7, 11.2, 19.7, 28.2, and 33.9 m from the inlet (Supplemental Figure S1). Woodchip

samples were collected along a center line at bottom depth (corresponding to the five porewater sampling points) and at 0.4 m above the bottom. Samples were also collected at depths of 11.2, 19.7, and 28.2 m at ± 1.35 m from the center line and 0.4 m above bottom (i.e., the deepest possible depth due to the trapezoidal shape of the reactor). At the inlet and outlet, woodchip samples were collected from the surface of the bioreactor. All samples were collected in triplicate. The samples were stored in sterile 50-ml plastic tubes and placed on ice for ~6 h following collection, frozen at -10°C for 4 d, and stored at -20°C until DNA extraction.

2.3 | Analyses

2.3.1 | Chemical analyses of water samples

We used porewater chemistry data from Nordström and Herbert (2018). Dissolved N_2O concentrations were determined via headspace equilibrium and analyzed at the Swedish University of Agricultural Sciences in Uppsala. The dissolved N_2O concentrations reported in this study differ from those reported in Nordström and Herbert (2018) because errors were identified in the latter study regarding the calculation of dissolved N_2O from headspace concentrations. See Nordström and Herbert (2018) for additional details on analytical methods.

2.3.2 | DNA extraction and quantitative real-time polymerase chain reaction

DNA from the Sterivex filter units was extracted using the MoBio PowerWater Sterivex DNA kit following the manufacturer’s instructions, including incubation at 90°C (MoBio Laboratories Inc., 2018). For DNA extraction from the woodchips (4 g) and sewage sludge (0.2 g), the DNeasy PowerMax Soil Kit was used according to the manufacturer’s instructions (Qiagen GmbH). Both the woodchips and digested sewage sludge were freeze-dried prior DNA extraction.

Real-time quantitative polymerase chain reaction (qPCR) was used to determine the abundances of functional genes specific for the denitrification, N_2O reduction, DNRA, and anammox pathways and used as proxies for the communities performing these reactions. Primers for *nirS* (Throbäck, Enwall, Jarvis, & Hallin, 2004) and *nirK* (Hallin & Lindgren, 1999; Henry et al., 2004) were used for the denitrifiers, *nosZI* (Henry, Bru, Stres, Hallet, & Philippot, 2006) and *nosZII* (Jones, Graf, Bru, Philippot, & Hallin, 2013) for the N_2O reducers, *hdh* (Schmid et al., 2008) for anammox bacteria, and *nrfA* (Mohan, Schmid, Jetten, & Cole, 2004; Welsh, Chee-Sanford, Connor, Löffler, & Sanford, 2014) for the DNRA communities. These primers, especially the ones

for *nir* and *nrfA*, do not cover the extant diversity of each gene (e.g., Bonilla-Rosso, Wittorf, Jones, & Hallin, 2016; Cannon, Sanford, Connor, Yang, & Chee-Sanford, 2019), which results in an underestimation of the absolute abundances. However, they allow for a comparative analysis of the relative abundance across samples by sampling a standard subset of each functional group for which functionality is verified (Penton et al., 2013).

The 16S rRNA gene (Muyzer, Dewaal, & Uitterlinden, 1993) was used as a proxy for the abundance of the total bacterial community. Each 15- μ l qPCR reaction contained 2–5 ng (water samples) or 0.1–0.3 ng (woodchip samples) of DNA, 0.25–2 μ M of each primer, 15 μ g bovine serum albumin, and 1x iQ SYBR Green Supermix (BioRad Laboratories). Two independent quantifications per gene were performed using the BioRad CFX Real-Time System (BioRad Laboratories). Potential PCR inhibition in the samples was tested by spiking each sample with the pGEM-T plasmid (Promega Co.) and amplifying it using plasmid-specific primers. Amplification was compared between samples and nonsample (water control) reactions, and no inhibition was present in the samples with the amounts of DNA extract used. Cycling protocols and primer concentrations are described in the supporting information (Supplemental Table S2).

2.3.3 | Statistical analysis and parameter estimation

Differences in the abundances of all functional genes and the 16S rRNA genes between porewater (including outlet samples), inlet water, woodchips, and sewage sludge were tested using Dunn's test, which is appropriate for groups with unequal numbers of observations (Zar, 2010), in R package 'FSA' (Dinno, 2017), which performs a Kruskal–Wallis test (normality could not be assumed based on a Shapiro–Wilks test; Supplemental Table S3) followed by pairwise comparisons. Corrections for multiple comparisons were done by false discovery rate (Benjamini & Hochberg, 1995). For comparisons between two groups, Wilcoxon rank sum tests were used.

Nonmetric multidimensional scaling (NMDS; using the R package 'vegan' [Oksanen et al., 2018]) was used to illustrate the structural differences in the concatenated N reducing communities (i.e., based on all functional genes) between samples from the porewater (including outlet samples), inlet water, woodchips, and the inoculum (digested sewage sludge). The abundances of the studied marker genes from each individual sample in the DWB were assumed to represent a specific N-reducing community. Gene abundances were square-root transformed and submitted to Wisconsin double standardization. Then, a community matrix with Bray–Curtis dissimilar-

ities was created and the NMDS was run with a maximum of 250 iterations.

We compared the similarity between the N reducing community in the porewater samples with those in the three potential sources: the inlet water, the woodchip media, and the inoculant sewage sludge. Community matrices based on Bray–Curtis dissimilarities were generated for each sample source using the same procedure as described above and compared using a permuted ($n = 999$) analysis of similarity (*anosim*; R-package 'vegan') (Oksanen et al., 2018).

To identify the selective pressures for changes in NO_2^- , N_2O , and NH_4^+ concentrations in the DWB, we first tested the correlation between porewater pH, temperature, and solute concentrations (NO_3^- , NO_2^- , N_2O , NH_4^+ , total organic C [TOC]) with the N reducing community structure in the porewater samples using a permuted ($n = 999$) correlation test (*envift*; R-package 'vegan') (Oksanen et al., 2018). Further, a Spearman's rank correlation analysis with permutation (10,000) tests (R-package 'coin') (Hothurn, Hornik, van de Wiel, & Zeileis, 2006) was used to correlate N species in the porewater with individual gene abundances and abundance ratios.

3 | RESULTS

3.1 | Porewater chemistry

The NO_3^- -N, NO_2^- -N, NH_4^+ -N, N_2O -N, and TOC concentrations as well as the C/ NO_3^- ratio (calculated from TOC and NO_3^- -N concentrations) are presented as a function of time, temperature, and position in the DWB (Figure 1). Nitrate concentrations consistently decreased along the DWB flowpath throughout the operational period (Figure 1a), with the lowest concentrations observed during the warmer periods (Days 1–85, 365–428). Nitrogen removal rates ranged from 0.14 to 37.5 g N m^{-3} (DWB volume) d^{-1} and have been previously shown to have a temperature dependence (Nordström & Herbert, 2019). Nitrite concentrations (Figure 1b) were observed up to 11 mg L^{-1} in the first half of the DWB during the first operational year but were below 1 mg L^{-1} in the DWB effluent with the exception of first week of operations. Similarly, NH_4^+ -N concentrations were elevated throughout the DWB during the first operational year (Figure 1c) but remained relatively constant at <0.5 mg L^{-1} during the second operational year. Nitrous oxide (Figure 1d) varied irregularly with sampling position and time but with a tendency for higher concentrations in the first half of the DWB during the summer months (Days 400 and 428). Nitrous oxide production rates, determined from the difference in inlet and outlet N_2O -N concentrations, ranged from ~0 to 3.7 mg N_2O -N m^{-3} d^{-1} ; this can be compared with a production in the range of 12–152 mg

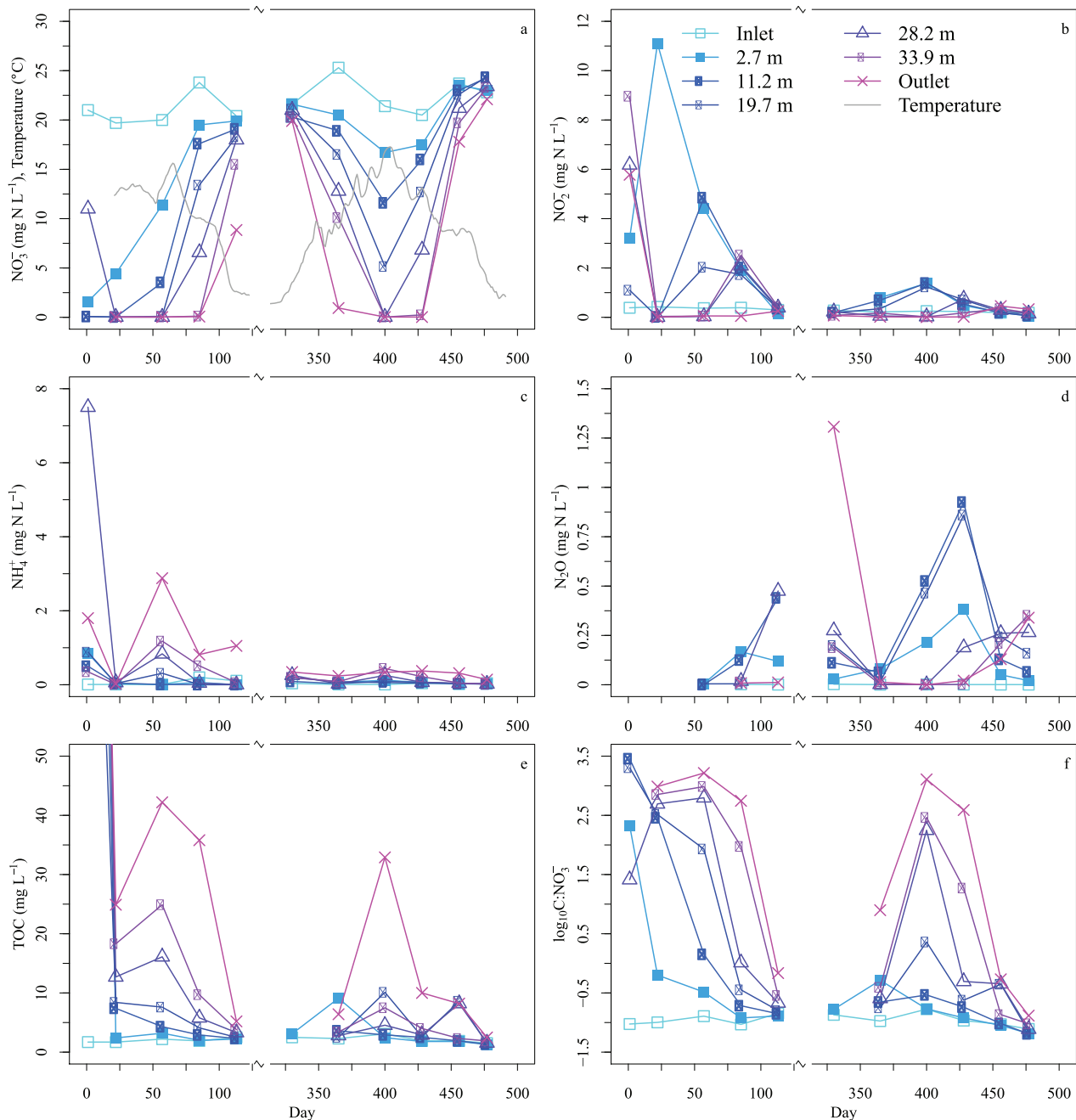


FIGURE 1 Porewater chemistry in the bioreactor. Concentrations of (a) NO_3^- -N, (b) NO_2^- -N, (c) NH_4^+ -N, (d) N_2O -N, (e) total organic C (TOC), and (f) $\log_{10}(\text{TOC}/\text{NO}_3^-)$ -N ratio as a function of time and position in the bioreactor. Position refers to distance from bioreactor inlet. On Day 1, TOC concentrations were 138–244 mg L⁻¹ (inlet excluded).

N_2O -N m⁻³ d⁻¹ for DWB's with much shorter HRTs (2–16 h) and composed of hardwood woodchips (Davis et al., 2019). As demonstrated in the porewater data, the average concentrations and concentration ranges of denitrification products (i.e., NO_2^- -N, N_2O -N) when combined from all positions were significantly different between the first and second operational year (Supplemental Figure S2).

Total organic C concentrations generally decreased during the first operational year and remained <10 mg L⁻¹ during the second year (with the exception of one sample; Figure 1e). The resultant TOC/ NO_3^- ratio (Figure 1f) exhibited increasing values with travel distance through the DWB and during the summer months, reflecting primarily the variations in NO_3^- -N concentration.

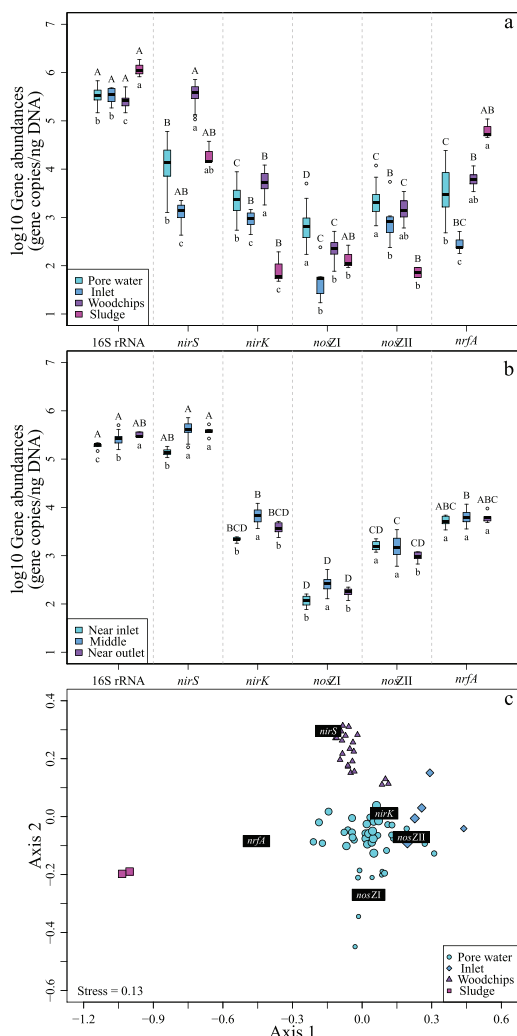


FIGURE 2 Abundances of the 16S rRNA gene and the functional genes *nirS*, *nirK*, *nosZI*, *nosZII*, and *nrfA* in bioreactor samples. (a) Gene abundances in porewater ($n = 47$ – 54), inlet water ($n = 7$), woodchips corresponding to the porewater sampling points and outlet ($n = 18$), and digested sewage sludge used as inoculum ($n = 2$ – 3) across the two operational years. Based on Dunn’s test ($p < .05$), uppercase letters indicate differences in gene abundances within sample type, and lowercase letters indicate differences in gene abundance compared with the respective gene abundance in other sample sources. (b) Gene abundances in woodchip samples from 0 m (bottom) and 0.4 m above bottom in the bioreactor, with data from the two depths combined. “Near inlet” ($n = 6$) and “Near outlet” ($n = 6$) indicate samples from 2.7 and 33.9 m from the inlet, along the center line (see Supplemental Figure S1); “Middle” ($n = 36$) indicates samples from 11.2, 19.7, and 28.2 m from inlet, at both depths along the centerline and at 0.4 m depth along the sides of the reactor (± 1.35 m from centerline). Based on Dunn’s test ($p < .05$), uppercase letters indicate differences in gene abundances within each position, and lowercase letters indicate differences in gene abundance compared with the respective gene abundance in other positions. In (a) and (b), empty circles are outliers and lines through boxes signifies median. (c) Nonmetric multidimensional scaling ordination based on Bray–Curtis dissimilarities for the abundances of the functional genes in porewater, inlet water, woodchips (from bottom centerline, inlet, and outlet), and digested sewage sludge used as inoculum. For water samples,

3.2 | Gene abundances and N-reducing community structure

The abundances of the total bacterial community and genes coding for the different N reducing pathways differed among sample types, but the *hdh* gene coding for anammox was not detected in any of the samples (Figure 2a). An assessment of the difference between woodchip samples collected at different depths indicated that there was not a significant difference ($p < .05$, one-sided Wilcoxon test) in the abundances of the 16S rRNA genes and the functional genes between the two sampling depths, with the exception of *nirS*. For *nirS*, there were significantly lower abundances at the bottom compared with 0.4 m above ($p < .01$) (data not shown). Regardless, woodchip samples from these two sample depths are considered together for the rest of this study.

There were significant differences in the abundances of the 16S rRNA and functional genes between the porewater, inlet water, woodchips, and digested sewage sludge (Figure 2a; Supplemental Table S4). The sample source with the highest abundance of functional genes differed depending on the gene, although gene abundances in the inlet water were most often the lowest among the different sample sources (Figure 2a). For the different genes and sample sources, *nirS* was most abundant in the woodchips and sludge, whereas *nrfA* in sludge had the greatest abundance. Among the woodchip samples, the 16S rRNA and *nirS* abundance varied the most along the flowpath from inlet to outlet and the *nrfA* abundance did not vary (Figure 2b). *nirK* and *nosZI* displayed the same pattern with the highest abundances in the middle section of the reactor, whereas *nirS* and *nosZII* had contrasting patterns, with *nirS* lower at the inlet and *nosZII* lower at the outlet.

The NMDS analysis (Figure 2c) showed that *nirS*-type denitrifiers were indicative of the N-reducing community structure in the woodchip media. By contrast, *nosZI* and *nosZII* involved in N₂O reduction were relatively more enriched in the porewater and inlet water samples in comparison to the woodchip media (Figure 2c), and *nrfA* (DNRA) characterized the N-reducing community in the digested sewage sludge.

Despite differences in absolute abundances, the distribution of gene abundances relative to each other in the porewater was comparable with that in the woodchip media ($nirS > nrfA \geq nirK > nosZII > nosZI$) (Figure 2a). However, when comparing the N-cycling community in porewater at Day 477 and woodchip samples from Day 490, there was a significant difference between these two sample pools ($R = .87$; $p = .001$), demonstrating that these two matrices represent different sampling environments.

increasing symbol sizes imply later sampling dates. Gene names in black boxes denote species scores

3.3 | Temporal changes in the N-reducing community and associated biogeochemical changes in the porewater

We observed differences in gene abundances between the operational years and along the flowpath of the DWB (Figure 3). In general, there was a significant increase in gene abundance between the corresponding periods in the first and second operational year with respect to *nirS*, *nirK*, *nosZII*, and *nrfA*, whereas the total bacterial community remained approximately the same and *nosZI* decreased significantly (Supplemental Figures S2 and S3). However, the opposite changes in *nosZI* and *nosZII* abundances more or less canceled out the total change in potential N₂O reduction capacity between years. The structure of the N reducing community in the porewater also changed over time and differed between the two operational years, as shown with NMDS (Figure 4), and the change was significantly associated with changes in porewater concentrations of NO₃⁻-N ($R^2 = .34$; $p = .001$), NO₂⁻-N ($R^2 = .30$; $p = .003$), N₂O-N ($R^2 = .17$; $p = .022$), NH₄⁺-N ($R^2 = .14$; $p = .040$), TOC ($R^2 = .28$; $p = .003$), DWB temperature ($R^2 = 0.46$; $p = .001$; see also Figure 2), and TOC/NO₃⁻ ratio ($R^2 = .3627$; $p = .001$) but not with porewater pH ($R^2 = .01$; $p = .901$). The differences in the structure of the N reducing community between years were mainly split in relation to axis 1 (Figure 4), corresponding to changes in the porewater concentrations of NO₂⁻-N and N₂O-N. Although there was no significant difference in the TOC/NO₃⁻ ratio between the two operational years (Supplemental Figure S2), the NMDS demonstrates that the TOC/NO₃⁻ ratio is likely controlled by DWB temperature (Figure 4).

Because the gene abundance data from the first operational year were limited to three sampling dates, it was not possible to make conclusive interpretations of temporal trends during the first year. The investigation of temporal changes over an operational year was hence restricted to data from the second year. During this period, gene copies representing the total bacterial community (Figure 3a) decreased in abundance by approximately 50%. Maximum gene abundances were observed during the summer months (Days 400 and 428) for *nirS* and *nrfA* and to a certain extent *nirK*, whereas *nosZII* abundance decreased and *nosZI* was relatively constant over this period (see Figure 3a–f). Indeed, abundances of *nrfA* closely followed porewater temperature variations during the second year, with the greatest covariation existing for sampling points towards the outlet (Figure 3f). The abundances of *nirS* also followed porewater temperature variations, but the peak in abundance appeared to lag behind the temperature maximum (Figure 3b). However, contrary to *nrfA*, *nirS* abundance peaked at locations in the first half of the DWB and increased nearest the outlet toward the end of the sampling period.

Among the investigated genes coding for NO₂⁻ reductases in denitrifiers (i.e., *nirS*, *nirK*), the abundance of *nirS* consistently exceeded that of *nirK* in the porewater (Figure 3b,c). The *nirS/nirK* ratio attained a maximum value at locations close to the inlet and during the summer months (data not shown). Relative to *nrfA*, the abundance of *nirS* + *nirK* was consistently greater during the two operational years (Figure 3g), with the exception of Day 400 near the outlet where *nrfA* > *nirS* + *nirK*. The abundance of *nirS* and *nirK* genes was also greatly in excess of the sum of the genes coding for N₂O reductase (i.e., *nosZI*, *nosZII*; Figure 3h).

Correlation analyses using data from the second year indicated that significant correlations ($r_s > |0.6|$; $p < .05$) existed among geochemical parameters and between geochemical parameters and gene abundances (Table 1). For example, N₂O correlated positively with NO₂⁻ and negatively with pH. Both NO₂⁻ and N₂O correlated with *nirS* and the $\Sigma nir/\Sigma nos$ ratio. The dominance of *nirS* over *nirK* was positively correlated with NO₂⁻, NO₃⁻, and N₂O. The TOC/NO₃⁻ ratio correlated with *nirK*, *nrfA*, NH₄⁺, and temperature, and *nrfA* was positively correlated with temperature, NH₄⁺, and TOC and negatively correlated with NO₃⁻. The ratio (*nirS* + *nirK*)/*nrfA* correlated positively with NO₃⁻-N and negatively with TOC/NO₃⁻.

4 | DISCUSSION

The higher abundance of functional genes involved in the denitrification pathway compared with DNRA and the absence of anammox in both the porewater and woodchip media agrees with denitrification being the major pathway for NO₃⁻ reduction and N removal in the DWB studied here (Nordström & Herbert, 2018) as well as in DWBs in general (Schipper et al., 2010). Based on gene abundance data, the structures of the N-reducing communities in the woodchips, sludge, inlet water, and the porewater were significantly different from one another in many instances. The original intention of inoculating with digested sewage sludge was to promote the rapid development of a denitrifying community in the woodchip material. However, the sludge also provided a high-abundance source of organisms with the *nrfA* gene (i.e., genetic capacity for DNRA, an undesired side-reaction in a denitrifying bioreactor). The gene abundances determined in the woodchip samples on Day 490 likely reflect the accumulated contribution from the sludge inoculant, the original community in the woodchips (not analyzed), the inlet water, and the temporal changes of the community in response to selective pressures. However, development of the N-reducing community is mainly determined by the type of substrate used in reactors (Hellman et al., 2020) and, as shown in Figure 4, the porewater TOC concentration, the TOC/NO₃⁻ ratio, and DWB temperature.

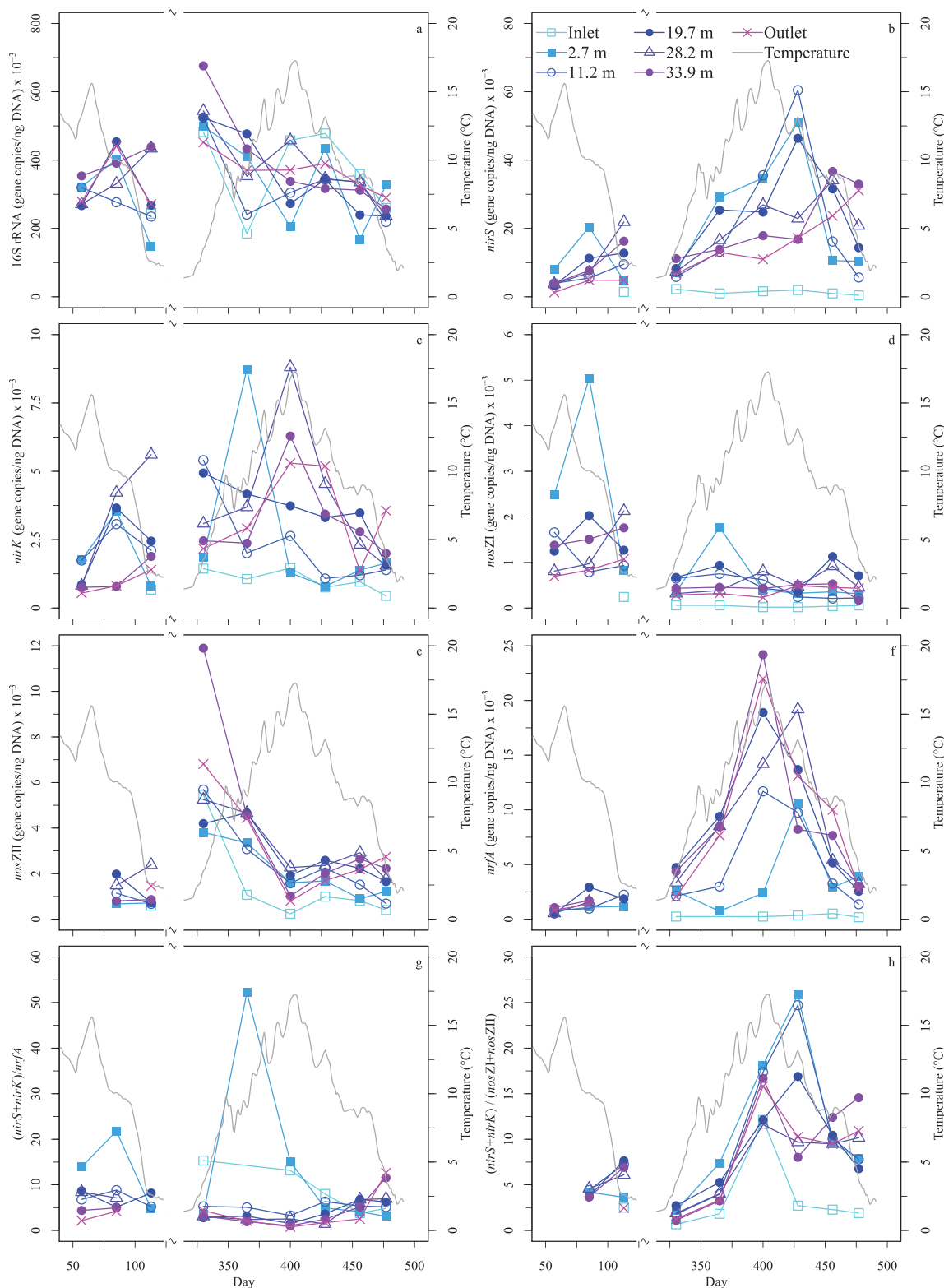


FIGURE 3 Gene abundances (a–f) and gene abundance ratios (g and h) as a function of time since start of denitrifying woodchip bioreactor operations and as a function of distance from the inlet. Abundances of (a) 16S rRNA genes and functional genes (b) *nirS*, (c) *nirK*, (d) *nosZI*, (e) *nosZII*, and (f) *nrfA*. Ratios (g) $(nirS + nirK)/nrfA$ (h) and $(nirS + nirK)/(nosZI + nosZII)$. Bioreactor temperature is plotted on secondary y axis. The x axis corresponds to day of porewater sampling (Days 57, 85, 113, 330, 365, 400, 428, 456, and 477)

TABLE 1 Spearman's rank correlation between chemistry, temperature, gene abundances, and ratios of different gene abundances in the porewater (bioreactor centerline)

	$\text{NO}_3\text{-N}$	$\text{NO}_2\text{-N}$	$\text{N}_2\text{O-N}$	$\text{NH}_4\text{-N}$	TOC	TOC/NO_3^-	pH	Temperature	<i>nirS</i>	<i>nirK</i>	<i>nosZI</i>	<i>nosZII</i>	<i>nrfA</i>
$\text{NO}_3\text{-N}$	–												
$\text{NO}_2\text{-N}$		–	.7***						.62***				–.8***
$\text{N}_2\text{O-N}$			–			–.38*	–.66***		.71*	–.42*			
$\text{NH}_4\text{-N}$				–	.64***	.79***	.49*		.47*				.56*
TOC					–	.93***	.56*	.55*	.65***	.4*			.49*
TOC/NO_3^-					–	–	.6*	.69***	.69***				.65***
pH						–	–		.52*				
Temperature							–	–	.26*			–.05*	.70***
<i>nirS</i>									–				.18*
<i>nirK</i>										–	.43*		.45*
<i>nosZI</i>											–		
<i>nosZII</i>												–	
<i>nrfA</i>													–
<i>nirS/nirK</i>	.46*	.58*	.8*	–.33*	–.41*	–.5*	–.59*	–.23*	.61***	–.75***	–.15*	–.03*	–.21*
<i>nosZII/nosZI</i>	–.13*	.09*	.17*	–.03*	–.19*	–.13*	.06*	–.05*	.14*	–.23*	–.49*	.45*	.13*
$\Sigma\text{nir}/\text{nrfA}$.75***	.37*	.55*	–.49*	–.43*	–.61***	–.51*	–.52*		–.45*			–.78***
$\Sigma\text{nir}/\Sigma\text{nosZ}$	–.19*	.29*	.53*	.23*	–.01*	.05*	–.52*	.44*	.67***	–.09*	–.27*	–.42*	.38*

Note. Only data from second operational year used. Empty cells indicate not significant. TOC, total organic C.

* Significant at the .05 probability level.

*** Significant at the .001 probability level.

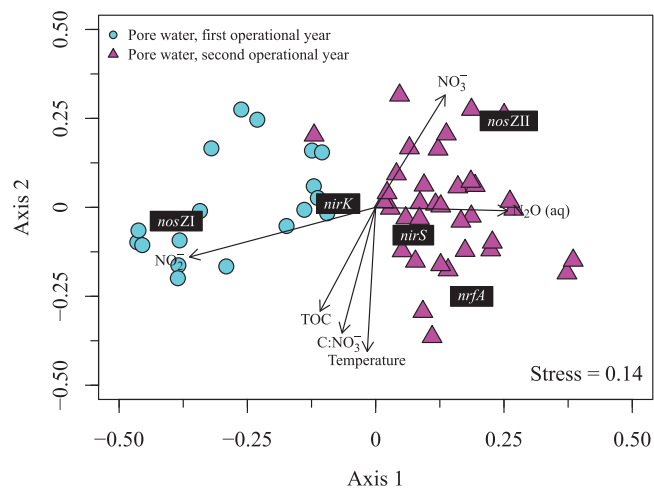


FIGURE 4 Nonmetric multidimensional scaling ordination based on Bray–Curtis dissimilarities for the abundance of the functional genes *nirS*, *nirK*, *nosZI*, *nosZII*, and *nrfA* in porewater samples. Arrows show significant correlations ($p < .05$) between the N cycling community structure across samples and porewater chemistry. Gene names in black boxes denote species scores. TOC, total organic C

The surface-bound N reducing community associated with the woodchips and containing *nirS*, *nirK*, and *nosZI* increased in abundance from the bioreactor inlet to the middle of the DWB (Figure 2b), suggesting that environmental conditions promoting the growth of organisms with *nirS*, *nirK*, and *nosZI* were better in the central region of the DWB compared with conditions closer to the inlet. A similar spatial development in gene abundance was observed in the porewater on Day 477, just prior to woodchip sampling (i.e., *nirS* and *nirK* gene abundances increased through bioreactor). Because temperature did not vary greatly within the bioreactor for any given date (data not shown), the increase in *nirS* and *nirK* gene abundances along the bioreactor flowpath was likely controlled by the relatively low concentration of organic C, elevated concentrations of NO_3^- and NO_2^- , and consequently the low TOC/ NO_3^- ratio (Figure 1f). These results are contrary to our previous study (Herbert et al., 2014) that indicated a decrease in *nirS* abundance in a sawdust DWB with distance from the bioreactor inlet; however, this system (Herbert et al., 2014) was NO_3^- limited in regions further from the inlet but was not C limited (i.e., high TOC/ NO_3^- ratio).

Based on the porewater samples (Figures 2 and 3), we clearly detected a shift in the structure of the N reducing community over time, as characterized by the change in the relative abundances of functional groups (Figure 3; Supplemental Figure S2). The increased abundance of the capacity for NO_2^- reduction relative to N_2O reduction during the second operational year suggests a preferential selection of *nirS*-type denitrifiers with a truncated denitrifying pathway terminating with N_2O . Dissolved N_2O porewater concentrations were most strongly correlated (Table 1) with pH and the type of

NO_2^- reductase (positively with *nirS* and *nirS/nirK* ratio and negatively with *nirK*; c.f. Barrett et al., 2016; Jones et al., 2014) and also with the relative abundance of NO_2^- reducers to N_2O reducers ($\Sigma\text{nir}/\Sigma\text{nosZ}$). Furthermore, the abundances of *nirS* and *nirK* (and also *nrfA*) during the second operational year (Figure 3) demonstrated a clear temperature dependence, whereas abundances of *nosZI* and *nosZII* appeared to be independent of temperature, which led to a correlation between temperature and $\Sigma\text{nir}/\Sigma\text{nosZ}$ (Table 1). Warneke, Schipper, Bruesewitz, McDonald, and Cameron (2011a) showed that an increased abundance of NO_2^- reducers over N_2O reducers at higher temperatures, including a relative enrichment in *nirS*-type to *nirK*-type denitrifiers, was associated with increased N_2O emissions in denitrifying bioreactors. Our observations imply an increased genetic potential for the production of N_2O from DWBs over time and with increasing temperature at HRTs of 1–2.6 d. In addition, the genetic potential for N_2O production was spatially variable within the bioreactor, implying a geochemical control (e.g., TOC/ NO_3^- , see below) as well. These implications are important contributions to our general understanding of greenhouse gas emissions from DWBs over longer time scales because they indicate the importance of understanding the temporal development of these systems.

The preferential promotion of denitrifiers with a denitrification pathway terminating with N_2O may have been an effect of the increased competition for electron donors. The simulations by Nordström and Herbert (2018) suggested a decrease in the export of acetate from the DWB studied here with time from start-up, which is consistent with the observations of other studies (Grießmeier & Gescher, 2018; Grießmeier et al., 2017). When there is competition for available organic C by denitrifiers capable of complete denitrification, electrons are preferentially directed to the NO_2^- reductase rather than the N_2O reductase (Pan et al., 2013). This suggests that low TOC/ NO_3^- ratios could lead to the preferential promotion of microorganisms with denitrification pathways truncated to N_2O , in this case *nirS* denitrifiers. This was supported in this study by the negative correlation between TOC/ NO_3^- ratio and the *nirS/nirK* ratio and its positive correlation with *nirK* abundances. Promotion of organisms lacking the *nosZ* gene is also supported by the spatially dependent relationship between N_2O concentrations and $\Sigma\text{nir}/\Sigma\text{nosZ}$ (Figures 1d and 3h). Further, clade II *nosZ* is frequently associated with nondenitrifying bacteria that do not have the genetic make-up needed for N_2O production (Graf et al., 2014; Jones et al., 2014). The disproportional abundance of *nos* and *nir* genes suggests that the denitrification pathway is split among community members. This decoupling of the intermediate steps of denitrification onto several populations would reduce intraorganism competition (Lilja & Johnson, 2016; Pan et al., 2013). Such decoupling and metabolic specialization among truncated denitrifiers and N_2O reducers has been inferred from

metagenomes in tidal sediments and grassland soils (Diamond et al., 2019; Marchant et al., 2018).

The abundance of *nrfA* genes detected in the porewater suggests DNRA bacteria may be competing for NO_3^- with the denitrifiers (Figures 2a and 3f). The genetic potential for NO_2^- reduction relative to DNRA (i.e., $\Sigma\text{nir}/\text{nrfA}$) was negatively correlated with the TOC/NO_3^- ratio (Table 1), in agreement with studies showing that DNRA is favored by high C/N ratios (e.g., Kraft et al., 2014). Both temperature and the TOC/NO_3^- ratio had an important control on *nrfA* abundance (Figure 3f) and hence NH_4^+-N concentrations, as indicated by significant correlations between these parameters (Table 1). However, the NH_4^+ concentrations were overall low, suggesting limited importance of this unwanted process. Interestingly, many DNRA bacteria are also fermenting (Muyzer & Stams, 2008; Van Den Berg, Elisário, Kuenen, Kleerebezem, & van Loosdrecht, 2017), and hence the DNRA bacteria may also contribute to fermentation and thereby support denitrification despite being competitors for NO_3^- .

5 | CONCLUSIONS

Denitrification was the major pathway for NO_3^- reduction and N removal in the DWB over two operational years at HRTs of 1–2.6 d but was associated with an increased genetic potential for N_2O production with time. We conclude that pH and temporal and spatial changes in the relative abundance of different denitrifier genotypes, indicated by abundances of genes involved in different steps in the denitrification pathway, controlled porewater concentrations of N_2O . Bioreactor temperature and TOC/NO_3^- ratio had a strong control on the occurrence of bacteria capable of NO_2^- reduction and those capable of DNRA (preferring high TOC/NO_3^-). A spatially variable community, likely dominated by *nirS*-type denitrifiers with a truncated pathway terminating with N_2O , developed over time in the DWB, where the supply of electron donors from substrate decomposition may be a controlling parameter on community development. Considering the significant differences in DWB chemistry and functional gene abundance between the two operational years, this study highlights the importance of distinguishing between initial variations during a start-up period, which may be extensive in length, and the long-term performance of a DWB.

ACKNOWLEDGMENTS

This work was supported by the Luossavaara-Kiirunavaara Aktiebolag (LKAB) and VINNOVA, The Swedish Innovation Agency, under Grant 2014–011334. The authors thank Christopher Jones, Carlos Palacin-Lizarbe, and Robert Almstrand for help related to the use of Sterivex filter units. The authors thank the anonymous reviewers for all their comments and advice.

CONFLICT OF INTEREST

There are no conflicts of interest.

ORCID

Albin Nordström  <https://orcid.org/0000-0002-0311-8368>

Roger B. Herbert  <https://orcid.org/0000-0002-7561-757X>

REFERENCES

- Barrett, M., Khalil, M. I., Jahangir, M. M. R., Lee, C., Cardenas, L. M., Collins, G., ... O'Flaherty, V. O. (2016). Carbon amendment and soil depth affect the distribution and abundance of denitrifiers in agricultural soils. *Environmental Science and Pollution Research*, 23, 7899–7910. <https://doi.org/10.1007/s11356-015-6030-1>
- Benjamini, Y., & Hochberg, Y. (1995). Controlling the false discovery rate: A practical and powerful approach to multiple testing. *Journal of the Royal Statistical Society Series B-Methodological*, 57(1), 289–300.
- Bonilla-Rosso, G., Wittorf, L., Jones, C. M., & Hallin, S. (2016). Design and evaluation of primers targeting genes encoding NO-forming nitrite reductases: Implications for ecological inference of denitrifying communities. *Scientific Reports*, 6, 39208. <https://doi.org/10.1038/srep39208>
- Cameron, S. G., & Schipper, L. A. (2010). Nitrate removal and hydraulic performance of organic carbon for use in denitrification beds. *Ecological Engineering*, 36(11), 1588–1595. <https://doi.org/10.1016/j.ecoleng.2010.03.010>
- Cannon, J., Sanford, R. A., Connor, L., Yang, W. H., & Chee-Sanford, J. (2019). Optimization of PCR primers to detect phylogenetically diverse *nrfA* genes associated with nitrite ammonification. *Journal of Microbiological Methods*, 160, 49–59. <https://doi.org/10.1016/j.mimet.2019.03.020>
- Davis, M. P., Martin, E. A., Moorman, T. B., Isenhardt, T. M., & Soupir, M. L. (2019). Nitrous oxide and methane production from denitrifying woodchip bioreactors at three hydraulic residence times. *Journal of Environmental Management*, 242, 290–297. <https://doi.org/10.1016/j.jenvman.2019.04.055>
- Diamond, S., Andeer, P. F., Li, Z., Crits-Christoph, A., Burstein, D., Anantharaman, K., ... Banfield, J. F. (2019). Mediterranean grassland soil C-N compound turnover is dependent on rainfall and depth, and is mediated by genomically divergent microorganisms. *Nature Microbiology*, 4(8), 1356–1367. <https://doi.org/10.1038/s41564-019-0449-y>
- Dinno, A. (2017). *Dunn.test: Dunn's test of multiple comparisons using rank sums*. R package version 1.3.5. Retrieved from <https://CRAN.R-project.org/package=dunn.test>
- Elgood, Z., Robertson, W. D., Schiff, S. L., & Elgood, R. (2010). Nitrate removal and greenhouse gas production in a stream-bed denitrifying bioreactor. *Ecological Engineering*, 36(11), 1575–1580. <https://doi.org/10.1016/j.ecoleng.2010.03.011>
- Felgate, H., Giannopoulos, G., Sullivan, M. J., Gates, A. J., Clarke, T. A., Baggs, E., ... Richardson, D. J. (2012). The impact of copper, nitrate and carbon status on the emission of nitrous oxide by two species of bacteria with biochemically distinct denitrification pathways. *Environmental Microbiology*, 14(7), 1788–1800. <https://doi.org/10.1111/j.1462-2920.2012.02789.x>
- Feyereisen, G. W., Moorman, T. B., Christianson, L. E., Venterea, R. T., Coulter, J. A., & Tschirner, U. W. (2016). Performance of agricultural residue media in laboratory denitrifying bioreactors at low

- temperatures. *Journal of Environmental Quality*, 45(3), 779–787. <https://doi.org/10.2134/jeq2015.07.0407>
- Graf, D. R. H., Jones, C. M., & Hallin, S. (2014). Intergenomic comparisons highlight modularity of the denitrification pathway and underpin the importance of community structure for N₂O emissions. *PLOS ONE*, 9(12), e114118. <https://doi.org/10.1371/journal.pone.0114118>
- Greenan, C. M., Moonman, T. B., Kaspar, T. C., Patkin, T. B., & Jaynes, D. B. (2006). Comparing carbon substrates for denitrification of subsurface drainage water. *Journal of Environmental Quality*, 35, 824–829. <https://doi.org/10.2134/jeq2005.0247>
- Grieblmeier, V., Bremges, A., McHardy, A. C., & Gescher, J. (2017). Investigation of different nitrogen reduction routes and their key microbial players in wood chip-driven denitrification beds. *Scientific Reports*, 7, 17028. <https://doi.org/10.1038/s41598-017-17312-2>
- Grieblmeier, V., & Gescher, J. (2018). Influence of the potential carbon sources for field denitrification beds on their microbial diversity and the fate of carbon and nitrate. *Frontiers in Microbiology*, 9, 1313. <https://doi.org/10.3389/fmicb.2018.01313>
- Hallin, S., & Lindgren, P.-E. (1999). PCR detection of genes encoding nitrite reductase in denitrifying bacteria. *Applied and Environmental Microbiology*, 65(4), 1652–1657.
- Hallin, S., Philippot, L., Löffler, F. E., Sanford, R. A., & Jones, C. M. (2018). Genomics and ecology of novel N₂O-reducing microorganisms. *Trends in Microbiology*, 26(1), 43–55. <https://doi.org/10.1016/j.tim.2017.07.003>
- Hellman, M., Hubalek, V., Juhanson, J., Almstrand, R., Peura, S., & Hallin, S. (2020). Substrate type determines microbial activity and community composition in bioreactors for nitrate removal by denitrification at low temperature. *Science of the Total Environment*. <https://doi.org/10.1016/j.scitotenv.2020.143023>.
- Henry, S., Baudoin, E., López-Gutiérrez, J. C., Martin-Laruent, F., Brauman, A., & Philippot, L. (2004). Quantification of denitrifying bacteria in soils by *nirK* gene targeted real-time PCR. *Journal of Microbiological Methods*, 59(3), 327–335. <https://doi.org/10.1016/j.mimet.2004.07.002>
- Henry, S., Bru, D., Stres, B., Hallet, S., & Philippot, L. (2006). Quantitative detection of the *nosZ* gene, encoding nitrous oxide reductase, and comparison of the abundances of 16S rRNA, *narG*, *nirK*, and *nosZ* genes in soils. *Applied and Environmental Microbiology*, 72(8), 5181–5189. <https://doi.org/10.1128/AEM.00231-06>
- Herbert, R. B., Winbjörk, H., Hellman, M., & Hallin, S. (2014). Nitrogen removal and spatial distribution of denitrifier and anammox communities in a bioreactor for mine drainage treatment. *Water Research*, 66, 350–360. <https://doi.org/10.1016/j.watres.2014.08.038>
- Hothurn, T., Hornik, K., van de Wiel, M. A., & Zeileis, A. (2006). A lego system for conditional inference. *American Statistician*, 60(3), 257–263. <https://doi.org/10.1198/000313006>
- Jones, C. M., Graf, D. R. H., Bru, D., Philippot, L., & Hallin, S. (2013). The unaccounted yet abundant nitrous oxide-reducing microbial community: A potential nitrous oxide sink. *ISME Journal*, 7(2), 417–426. <https://doi.org/10.1038/ismej.2012.125>
- Jones, C. M., Spor, A., Brennan, F. P., Breuil, M. C., Bru, D., Lemanceau, P., ... Philippot, L. (2014). Recently identified microbial guild mediates soil N₂O sink capacity. *Nature Climate Change*, 4, 801–805. <https://doi.org/10.1038/NCLIMATE2301>
- Kraft, B., Tegetmeyer, H. E., Sharma, R., Klotz, M. G., Ferdelman, T. G., Hettich, R. L., ... Strous, M. (2014). Nitrogen cycling: The environmental controls that govern the end product of bacterial nitrate respiration. *Science*, 345(6197), 676–679. <https://doi.org/10.1126/science.1254070>
- Lilja, E. E., & Johnson, D. R. (2016). Segregating metabolic processes into different microbial cells accelerates the consumption of inhibitory substrates. *The ISME Journal*, 10, 1568–1578. <https://doi.org/10.1038/ismej.2015.243>
- Marchant, H. K., Tegetmeyer, H. E., Ahmerkamp, S., Holtappels, M., Lavik, G., Graf, J., ... Kuypers, M. M. M. (2018). Metabolic specialization of denitrifiers in permeable sediments controls N₂O emissions. *Environmental Microbiology*, 20, 4486–4502. <https://doi.org/10.1111/1462-2920.14385>
- MoBio Laboratories Inc. (2018). *PowerWater® Sterivex™ DNA Isolation Kit instruction manual*. Retrieved from <https://www.qiagen.com/us/resources/resourcedetail?id=86fe0107-d78b-4a0d-b5fd-3c2cb414a749&lang=en>
- Mohan, S. B., Schmid, M., Jetten, M., & Cole, J. (2004). Detection and widespread distribution of the *nrfA* gene encoding nitrite reduction to ammonia, a short circuit in the biological nitrogen cycle that competes with denitrification. *FEMS Microbiology Ecology*, 49(3), 433–443. <https://doi.org/10.1016/j.femsec.2004.04.012>
- Muyzer, G., Dewaal, E. C., & Uitterlinden, A. G. (1993). Profiling of complex microbial populations by denaturing gradient gel electrophoresis analysis of polymerase chain reaction-amplified genes coding for 16S rRNA. *Applied and Environmental Microbiology*, 59(3), 695–700.
- Muyzer, G., & Stams, A. J. M. (2008). The ecology and biotechnology of sulphate-reducing bacteria. *Nature Reviews Microbiology*, 6(6), 441–454. <https://doi.org/10.1038/nrmicro1892>
- Nordström, A., & Herbert, R. B. (2017). Denitrification in a low-temperature bioreactor system at two different hydraulic residence times: Laboratory column studies. *Environmental Technology*, 38, 1362–1375. <https://doi.org/10.1080/09593330.2016.1228699>
- Nordström, A., & Herbert, R. B. (2018). Determination of major biogeochemical processes in a denitrifying woodchip bioreactor for treating mine drainage. *Ecological Engineering*, 110, 54–66. <https://doi.org/10.1016/j.ecoleng.2017.09.018>
- Nordström, A., & Herbert, R. B. (2019). Identification of the temporal control on nitrate removal rate variability in a denitrifying woodchip bioreactor. *Ecological Engineering*, 127, 88–95. <https://doi.org/10.1016/j.ecoleng.2018.11.015>
- Oksanen, J., Guillaume Blanchet, F., Friendly, M., Kindt, R., Legendre, P., McGlenn, D., ... Wagner, H. (2018). *vegan: Community ecology package*. R package version 2.5-2. Retrieved from <https://CRAN.R-project.org/package=vegan>
- Penton, C. R., Johnson, T. A., Quensen III J. F., Iwai, S., Cole, J. R., & Tiedje, J. M. (2013). Functional genes to assess nitrogen cycling and aromatic hydrocarbon degradation: Primers and processing matter. *Frontiers in Microbiology*, 4, 279. <https://doi.org/10.3389/fmicb.2013.00279>
- Pan, Y., Ni, B. J., Bond, P. L., Ye, L., & Yuan, Z. (2013). Electron competition among nitrogen oxides reduction during methanol-utilizing denitrification in wastewater treatment. *Water Research*, 47(10), 3273–3281. <https://doi.org/10.1016/j.watres.2013.02.054>
- Robertson, W. D. (2010). Nitrate removal rates in woodchip media of varying age. *Ecological Engineering*, 36(11), 1581–1587. <https://doi.org/10.1016/j.ecoleng.2010.01.008>
- Schipper, L. A., Robertson, W. D., Gold, A. J., Jaynes, D. B., & Cameron, S. C. (2010). Denitrifying bioreactors: An approach for reducing

- nitrate loads to receiving waters. *Ecological Engineering*, 36(11), 1532–1543. <https://doi.org/10.1016/j.ecoleng.2010.04.008>
- Schmid, M. C., Hooper, A. B., Klotz, M. G., Woebken, D., Lam, P., Kuypers, M. M. M., . . . Jetten, M. S. M. (2008). Environmental detection of octahaem cytochrome c hydroxylamine/hydrazine oxidoreductase genes of aerobic and anaerobic ammonium-oxidizing bacteria. *Environmental Microbiology*, 10(11), 31–40–3149. <https://doi.org/10.1111/j.1462-2920.2008.01732.x>
- Throbäck, I. N., Enwall, K., Jarvis, A., & Hallin, S. (2004). Reassessing PCR primers targeting nirS, nirK and nosZ genes for community surveys of denitrifying bacteria with DGGE. *FEMS Microbiology Ecology*, 49(3), 401–417. <https://doi.org/10.1016/j.femsec.2004.04.011>
- Van Den Berg, E. M., Elisário, M. P., Kuenen, J. G., Kleerebezem, R., & van Loosdrecht, M. C. M. (2017). Fermentative bacteria influence the competition between denitrifiers and DNRA bacteria. *Frontiers in Microbiology*, 8, 1684. <https://doi.org/10.3389/fmicb.2017.01684>
- Van Den Berg, E. M., Van Dongen, U., Abbas, B., & Van Loosdrecht, M. C. (2015). Enrichment of DNRA bacteria in a continuous culture. *The ISME Journal*, 9, 2153–2161. <https://doi.org/10.1038/ismej.2015.26>
- Warneke, S., Schipper, L. A., Bruesewitz, D. A., McDonald, I., & Cameron, S. (2011a). Rates, controls and potential adverse effects of nitrate removal in a denitrification bed. *Ecological Engineering*, 37(3), 511–522. <https://doi.org/10.1016/j.ecoleng.2010.12.006>
- Warneke, S., Schipper, L. A., Matiassek, M. G., Scow, K. M., Cameron, S., Bruesewitz, D. A., & McDonald, I. R. (2011b). Nitrate removal, communities of denitrifiers and adverse effects in different carbon substrates for use in denitrification beds. *Water Research*, 45(17), 5463–5475. <https://doi.org/10.1016/j.watres.2011.08.007>
- Welsh, A., Chee-Sanford, J. C., Connor, L. M., Löffler, F. E., & Sanford, R. A. (2014). Refined NrfA phylogeny improves PCR-Based nrfA gene detection. *Applied and Environmental Microbiology*, 80(7), 2110–2119. <https://doi.org/10.1128/AEM.03443-13>
- Yoon, S., Cruz-García, C., Sanford, R., Ritalahti, K. M., & Löffler, F. E. (2015). Denitrification versus respiratory ammonification: Environmental controls of two competing dissimilatory NO₃/NO₂ reduction pathways in *Shewanella loihica* strain PV-4. *The ISME Journal*, 9, 1093–1104. <https://doi.org/10.1038/ismej.2014.201>
- Zar, J. H. (2010). *Biostatistical analysis* (5th ed.). Upper Saddle River, NJ: Pearson Prentice Hall.

SUPPORTING INFORMATION

Additional supporting information may be found online in the Supporting Information section at the end of the article.

How to cite this article: Nordström A, Hellman M, Hallin S, Herbert RB. Microbial controls on net production of nitrous oxide in a denitrifying woodchip bioreactor. *J. Environ. Qual.* 2021;50:228–240. <https://doi.org/10.1002/jeq2.20181>